

1 **Quantifying the impact of riverine particulate dissolution in seawater on**
2 **ocean chemistry**

3 Morgan T. Jones¹, Sigurður R. Gislason², Kevin W. Burton³, Christopher R. Pearce⁴, Vasileios
4 Mavromatis⁵, Philip A.E. Pogge von Strandmann⁶ & Eric H. Oelkers^{2,6,7}

5 ¹ Centre of Earth Evolution and Dynamics (CEED), University of Oslo, Oslo, Norway

6 ² Institute of Earth Sciences, University of Iceland, Sturlugata 7, Reykjavík, Iceland

7 ³ Department of Earth Sciences, Durham University, Durham, UK

8 ⁴ School of Ocean and Earth Science, National Oceanography Centre, Southampton University,
9 European Way, Southampton, UK

10 ⁵ Graz University of Technology, Institute of Applied Geosciences, Rechbauerstraße 12, 8010
11 Graz, Austria

12 ⁶ Institute of Earth and Planetary Sciences, University College London and Birkbeck College
13 London, Gower Street, London, WC1E 6BT, UK

14 ⁷ GET-Université de Toulouse-CNRS-IRD-OMP, Toulouse, France

15

16 **Abstract**

17 The quantification of the sources and sinks of elements to the oceans forms the basis of our
18 understanding of global geochemical cycles and the chemical evolution of the Earth's surface.
19 There is, however, a large imbalance in the current best estimates of the global fluxes to the
20 oceans for many elements. In the case of strontium (Sr), balancing the input from rivers would

21 require a much greater mantle-derived component than is possible from hydrothermal water flux
22 estimates at mid-ocean ridges. Current estimates of riverine fluxes are based entirely on
23 measurements of dissolved metal concentrations, and neglect the impact of riverine particulate
24 dissolution in seawater. Here we present $^{87}\text{Sr}/^{86}\text{Sr}$ isotope data from an Icelandic estuary, which
25 demonstrate rapid Sr release from the riverine particulates. We calculate that this Sr release is
26 1.1-7.5 times greater than the corresponding dissolved riverine flux. If such behaviour is typical
27 of volcanic particulates worldwide, this release could account for 6-45 % of the perceived marine
28 Sr budget imbalance, with continued element release over longer timescales further reducing the
29 deficit. Similar release from particulate material will greatly affect the marine budgets of many
30 other elements, changing our understanding of coastal productivity, and anthropogenic effects
31 such as soil erosion and the damming of rivers.

32

33 **1. Introduction**

34 Continental weathering and erosion is the primary control on the transport of material from the
35 continents to the oceans, and a major component of the cycles of many elements on the Earth's
36 surface. The riverine flux of material from continental weathering is the dominant input of many
37 elements to the oceans. Ocean chemistry is commonly modelled as a combination of these
38 riverine fluxes, hydrothermal exchange at mid-ocean ridges, and sedimentation coupled to burial
39 (Riley & Chester, 1971). Strontium is among the best constrained of the global element cycles
40 over geologic time due to the facility of measuring its isotopic composition, its significant
41 temporal isotope variations, and its preferential incorporation into marine carbonates. The ratio
42 between the radiogenic ^{87}Sr (a product of the decay of ^{87}Rb) and stable ^{86}Sr isotopes increases
43 with the age of the rock substrate. The $^{87}\text{Sr}/^{86}\text{Sr}$ isotope composition and Sr concentrations of

44 | the open oceans is currently homogenous at ~0.7092 (Elderfield, 1986) and ~7.85 mg/L (Bernat
45 | et al., 1972), respectively, as the residence time of Sr greatly exceeds the rate of ocean mixing
46 | (Broecker & Peng, 1982). This value reflects a balance in inputs and outputs between radiogenic
47 | Sr derived from the continents and unradiogenic Sr from mantle-derived material. While
48 | spatially homogenous at current levels of precision, seawater $^{87}\text{Sr}/^{86}\text{Sr}$ has varied significantly
49 | over geological time (e.g. Veizer et al., 1999). These changes to seawater $^{87}\text{Sr}/^{86}\text{Sr}$ have been
50 | used to infer changes in inputs and outputs to the oceans in response to climatic and/or tectonic
51 | forcings over geological time (e.g. McArthur et al., 2001); although this is contentious (Palmer &
52 | Edmond, 1992; Oliver et al., 2003). Strontium isotope compositions have also been used as
53 | tracers of inputs from different river catchments into intra-continental seas (Andersson et al.,
54 | 1991).

55 |

56 | Seawater $^{87}\text{Sr}/^{86}\text{Sr}$ has been increasing at a rate of $0.000054 \text{ Myr}^{-1}$ in the Neogene and
57 | Pleistocene (Henderson et al., 1994; Hodell et al., 1989). There is a current discrepancy in our
58 | scientific understanding of the global Sr cycle, as mass balance calculations indicate that the
59 | current input of radiogenic Sr from the continents, assumed to only be transported in dissolved
60 | form to the oceans, cannot be balanced by unradiogenic Sr originating from hydrothermal
61 | exchange with oceanic crust to satisfy the observed rate of $^{87}\text{Sr}/^{86}\text{Sr}$ change. The global average
62 | dissolved riverine $^{87}\text{Sr}/^{86}\text{Sr}$ input is approximately 0.7136 (Allègre et al., 2010) while Sr liberated
63 | during hydrothermal exchange has a ratio of 0.7029 (Albarède et al., 1981). To balance the input
64 | from the world's rivers, the hydrothermal flux would need to be 4-20 times higher than current
65 | estimates (Davis et al., 2003; Hodell et al., 1989; Palmer and Edmond, 1989; Vance et al., 2009).

66 | A number of mechanisms have been proposed to reconcile this apparent flux imbalance. One

67 [possibility is](#) a deglacial weathering pulse that has yet to decay, [which means that current](#)
68 [dissolved riverine measurements would not be representative of the average over a time period](#)
69 [greater than glacial/interglacial cycles](#) (Vance et al., 2009). [Potential missing fluxes of](#)
70 [unradiogenic Sr include](#) groundwater inputs from volcanic terrains (Allègre et al., 2010) [and off-](#)
71 [axis exchange with oceanic crust \(Elderfield and Gieskes, 1982\), with the latter considered to be](#)
72 [of insufficient magnitude to play a considerable role \(Davis et al., 2003\).](#)

73

74 [Recent estimates](#) suggest that rivers transport between 15-20 Gt yr⁻¹ of suspended material to the
75 ocean each year (Peucker-Ehrenbrink et al., 2010; Walling, 2006), considerably greater than the
76 dissolved [riverine](#) and aeolian fluxes combined (Oelkers et al., 2011; 2012). Traditionally it has
77 been assumed that this particulate material undergoes little additional weathering in seawater,
78 because dissolution rates are reduced at low temperatures and because burial is thought to rapidly
79 isolate sediment. Nevertheless, some dissolution of riverine particulate material in the oceans is
80 inevitable, depending upon the saturation states of minerals in seawater, particulate surface area,
81 temperature, and prior weathering history. Experimental determinations of basalt dissolution
82 rates covering the pH and temperature range of modern seawater suggest that ~0.05 % of basaltic
83 particulate material [could](#) dissolve [in seawater](#) each day, with potentially profound impacts on
84 seawater chemistry (Gislason et al., 2006). More recently, laboratory experiments have shown
85 that there is substantial release of both soluble elements (such as Sr) and insoluble elements
86 (such as Nd) from riverine particulates to seawater over a timescale of days to months (Jones et
87 al., 2012a; 2012b; Pearce et al., 2013). [Field evidence also indicates that the dissolution of](#)
88 [particles is a significant part of the Nd cycle \(Lacan and Jeandel, 2005; Arsouze et al., 2009\),](#)
89 [including large submarine fans such as from the Ganges/Brahmaputra \(Singh et al., 2012\). For](#)

90 [more soluble elements such as Ca, Mg, and Sr, it is more difficult](#) to observe such release in
91 natural environments. [This is](#) due to [both their elevated](#) concentrations in seawater, [which are](#)
92 [several orders of magnitude greater than in the water arriving from estuaries,](#) and the effects of
93 contemporaneous precipitation of secondary minerals and ion-exchange [as river-transported](#)
94 [particles attempt to equilibrate with their new surroundings](#) (Jones et al., 2012a).

95
96 Here we present Sr elemental and isotope ($^{87}\text{Sr}/^{86}\text{Sr}$) data for riverine particulates from a basaltic
97 catchment, tracing their pathway from the Hvítá River into the Borgarfjörður Estuary in western
98 Iceland (Fig. 1). This catchment is well suited for the study of seawater-particulate interaction as
99 it has sparse vegetation, poorly developed soils, a stable climate, and a relatively homogenous
100 basaltic geology (c.f. Gislason et al., 1996). High physical erosions rates result in the delivery of
101 readily weathered material with a high surface area. The estuary is < 2 m deep over the first 5
102 km from the river mouth and is consequently tidally-dominated and both vertically and
103 horizontally well mixed. The shallow depth results in a high particulate-water ratio, maximizing
104 both the likelihood of continued particulate weathering, and a detectable chemical response in
105 the estuarine waters. The estuary has a natural narrowing, enhanced by Borgarfjörður Bridge at
106 Borgarnes (Fig. 1); consequently sediment input from outside the catchment is minimal.

107 Previous work [on this catchment](#) has demonstrated a distinct difference between the particulate
108 and dissolved compositions of several isotopes and elements including Sr (Jones et al., 2012a;
109 Pearce et al., 2010; 2013; Pogge von Strandmann et al., 2008). Crucially, [Li](#) isotope data
110 indicates that the [river-derived](#) particulates have experienced weathering in this estuary,
111 including both primary phase dissolution and secondary phase precipitation (Pogge von
112 Strandmann et al., 2008).

113

114 This study focuses on particle dissolution in a volcanic estuary for a number of reasons.
115 Estimates suggest that humid, young, and mountainous regions account for 40% of the global
116 dissolved flux and >60 % of the suspended particulate flux, despite comprising just 14 % of the
117 global drainage area (Milliman and Farnsworth, 2011). Proportionally, volcanic terrains exert a
118 much greater global influence on particulate fluxes to the oceans than expected from their
119 geographical extent, due to the combined effects of high relief, high runoff, the presence of
120 rapidly weathered volcanic rocks, and the absence of sedimentary traps (Milliman and Syvitski,
121 1992). The dissolution rates of primary basaltic minerals are, generally, an order of magnitude
122 or more rapid than those of granitic, metamorphic, or recycled sedimentary minerals (Dupré et
123 al., 2003; Gislason and Oelkers, 2003; Wolf-Boenisch et al., 2004; Gudbrandsson et al., 2012).
124 Moreover, particulate material delivered from volcanic islands typically undergoes little
125 weathering during riverine transport due to rapid transit to the oceans, so they are particularly
126 susceptible to dissolution [once they arrive in coastal waters](#). Hence, elemental release from
127 basaltic particles could potentially account for the imbalances identified in the global cycles of a
128 number of elements. For strontium, the $^{87}\text{Sr}/^{86}\text{Sr}$ isotope composition of basaltic particulates is
129 less radiogenic than seawater, and thus may potentially account for at least part of the apparent
130 shortfall in the marine Sr budget.

131

132 **2. Methods**

133 [2.1 Sampling](#)

134 Three field excursions were conducted in the Borgarfjörður/Hvítá catchment in 2003, 2008, and
135 2011. Samples were collected in transects along the estuary across the mixing zone of fresh and
136 saline water at high tide ([see](#) Fig. 1). The sampling methods from the 2003 field excursion are
137 summarized in Pogge von Strandmann et al. (2008). This sample suite, collected from the
138 Hvítárvellir Bridge to beyond the estuary mouth, represents a range in salinity from riverine
139 water to close to that of pure seawater. Fluid, suspended particles, and some colloid samples
140 were collected. The 2011 transect also started at Hvítárvellir and collected a higher density of
141 samples across the mixing zone, finishing at the bridge at Borgarnes. Surface water samples
142 were collected at a depth of 30 cm, with the exception of sample Bo8b, [which](#) was taken using a
143 Niskin sampler at a depth of 2 m (bottom water at this location). Conductivity and temperature
144 were measured on location. The samples were brought to the laboratory the same day and
145 filtered using a peristaltic pump through a 0.2 μm cellulose acetate membrane filter. The
146 samples were then subdivided prior to analysis. The filters were rinsed through with de-ionized
147 water, dried then weighed to estimate the suspended fraction [concentration](#).

148

149 The 2008 transect collected bedload material that has been the focus of previous investigations
150 (Jones et al., 2012a; Pearce et al., 2013). The sample locations matched that of the locations in
151 2003. In the shallow parts of the river and estuary, samples were collected from exposed
152 sandbanks or using a corer to collect material from the top 20 cm of the sediment. In deeper
153 water, samples were collected using a weighted bucket dragged behind the boat over a distance
154 of ~10 m. Repeat passes were conducted to [collect](#) sufficient material, which were then
155 homogenized prior to splitting into sample containers. All samples were dried at 40 °C
156 immediately after collection but no other processing was [performed](#).

157

158 2.2 Chemical Analyses

159 The filters and particulate material were flushed with 1L of de-ionized water and dried at 40 °C
160 before digestion in 20 ml savillex® containers at 120 °C for 72 hours using 2 ml 15M HNO₃.

161 After digestion, samples evaporated to dryness at 75 °C and re-diluted to 2 % HNO₃ prior to
162 elemental analyses. The elemental compositions of these samples after digestion were measured
163 in a Thermo Finnigan® ELEMENT XR at the GET in Toulouse, France. An In Re spike was
164 used for calibration purposes, and the total blank contributions (including blank filters) were
165 negligible for the elements presented in here compared to sample concentrations. Dissolved
166 concentrations of major elements and cations in collected fluid samples were conducted on an
167 ICP-SFMS in ALS laboratories, Sweden. Anion concentrations in these samples were measured
168 using ion chromatography techniques using a Dionex® ICS-2000 in Reykjavík, Iceland.

169

170 The ⁸⁷Sr/⁸⁶Sr ratios of each sample were measured using a VG Sector 54 thermal ionization mass
171 spectrometer (TIMS). Liquid and pre-digested solid samples were evaporated, taken up in 3M
172 HNO₃ and run through Sr-spec columns. The purified Sr was then loaded onto outgassed Ta
173 filaments. The samples were run at ⁸⁸Sr beam potentials of 2V and 100 ratios were collected
174 using a multi-dynamic peak jumping routine. Resulting ⁸⁷Sr/⁸⁶Sr ratios were normalized to an
175 ⁸⁶Sr/⁸⁸Sr ratio of 0.1194. Six analyses of the NBS 987 standard yielded an average ⁸⁷Sr/⁸⁶Sr of
176 0.710243 ± 0.000010 (2 SD). Individual errors did not exceed ± 0.000012 ⁸⁷Sr/⁸⁶Sr. Total
177 blanks for Sr were found to be negligible compared to the Sr amounts from the samples.

178

179 2.3 Mixing Calculations

180 This study focusses on the Sr isotope compositional evolution in Borgarfjörður estuary as river
 181 water mixes with seawater. The $^{87}\text{Sr}/^{86}\text{Sr}$ ratio of the estuary water in this system, if it was
 182 controlled by the mechanical mixing of two sources (the dissolved Sr present in the river and in
 183 seawater) would be given by:

$$185 \left(\frac{^{87}\text{Sr}}{^{86}\text{Sr}}\right)_{2comp} = \left(F_{river} \times \left(\frac{^{87}\text{Sr}}{^{86}\text{Sr}}\right)_{river}\right) + \left((1 - F_{river}) \times \left(\frac{^{87}\text{Sr}}{^{86}\text{Sr}}\right)_x\right) \quad \text{_____ (1)}$$

186 where $\left(\frac{^{87}\text{Sr}}{^{86}\text{Sr}}\right)_{2comp}$ refers to the isotopic ratio expected in the samples based on 2-component
 187 mechanical mixing. $\left(\frac{^{87}\text{Sr}}{^{86}\text{Sr}}\right)_{river}$ refers to the isotopic ratio of the Hvítá river end-member
 188 (0.70459), and $\left(\frac{^{87}\text{Sr}}{^{86}\text{Sr}}\right)_x$ refers to the isotopic value of non-riverine derived Sr, which in this case
 189 is equal to the isotopic ratio of seawater ($^{87}\text{Sr}/^{86}\text{Sr}_{sw} = 0.709198$). f_{river} refers to the fraction of
 190 dissolved riverine-derived Sr in the water, calculated from dissolved Cl concentrations:

$$192 f_{river} = \left(\frac{[Cl]_{est} - [Cl]_{sw}}{[Cl]_{river} - [Cl]_{sw}}\right) \times \left(\frac{[Cl]_{river}}{[Cl]_{est}}\right) \quad \text{_____ (2)}$$

193 where the suffixes *est*, *sw* and *river* refer to the estuarine sample, the river end-member, and the
 194 seawater end-member, respectively. The first part of the equation calculates the relative masses
 195 of the two water bodies, which is effectively ~1 in the low salinity mixing zone. The degree to
 196 which the Sr composition of Borgarfjörður estuarywater is consistent with the mechanical
 197 mixing of the dissolve Sr in the river and the seawater will be assessed in detail below.

199 **3. Results**

200 The measured element concentrations and $^{87}\text{Sr}/^{86}\text{Sr}$ ratios of all collected fluids are shown in
201 Table 1. The variation of estuary water Sr concentrations are plotted against the corresponding
202 Cl concentrations in Fig. 2. The solid line in this figure illustrates the mechanical mixing line
203 between river and sea water. Both sample sets plot close to the mechanical mixing line, with a
204 slight suggestion of a net removal of Sr in the low-salinity part of the mixing zone. Note that
205 there is a consistent difference in both elemental concentrations and $^{87}\text{Sr}/^{86}\text{Sr}$ ratio between the
206 2003 and 2011 samples at Hvítárvellir, which may indicate a greater input of sea-spray derived
207 Sr into the catchment in the 2003 samples.

208

209 The measured estuary fluid $^{87}\text{Sr}/^{86}\text{Sr}$ ratios are plotted as grey circles a function of the
210 corresponding aqueous Cl concentrations in Fig. 3. The solid curve in this figure illustrates the
211 Sr isotope compositions consistent with the mechanical mixing between river and estuary water
212 as calculated using Eqns. 1 and 2. Although the estuary water total Sr concentrations plotted in
213 Fig. 2 suggest close to conservative mixing of river and sea water, their $^{87}\text{Sr}/^{86}\text{Sr}$ ratios deviate
214 markedly from simple two-component mixing (Fig. 3). These same $^{87}\text{Sr}/^{86}\text{Sr}$ ratios are plotted as
215 a function of the fraction of river water component in the estuary water in Fig. 4. The
216 distribution of the symbols shows a clear deviation from the two component mixing line. The
217 difference between the observed and calculated two-component mixing $^{87}\text{Sr}/^{86}\text{Sr}$ values are
218 consistently more than an order of magnitude greater than the measurement error of ± 0.000012 ,
219 indicating that this is a robust and sizeable deviation from simple mixing. The difference
220 between the measured estuary water $^{87}\text{Sr}/^{86}\text{Sr}$ ratios and those estimated from a two component
221 mixing model are shown as a function of the corresponding Cl concentrations in Fig. 5. This
222 $^{87}\text{Sr}/^{86}\text{Sr}$ deviation is evident from a Cl concentration of approximately 50 mg/L. At its

223 maximum, the dissolved $^{87}\text{Sr}/^{86}\text{Sr}$ ratio in the mixing zone is 690 (± 135) and 3460 (± 920) ppm
224 (10^{-6}) lower than that predicted by conservative mixing in 2011 and 2003, respectively. Note the
225 considerably larger errors for the 2003 dataset are due to the inherent uncertainties of using a
226 riverine end-member from a different spot-sample set. Experimentally derived dissolution rates
227 of basaltic particulates from Icelandic catchments in seawater have shown both bedload and
228 suspended sediment from Icelandic river catchments react to change the seawater $^{87}\text{Sr}/^{86}\text{Sr}$
229 without a contemporaneous change in Sr concentrations over a period of days to months (Jones
230 et al., 2012a; 2012b). These laboratory dissolution rates after 1 to 4 days are shown as an
231 expected deviation from pure mechanical mixing in Fig. 5. Both the 2003 and 2011 sample sets
232 approach the calculated offset after just one day, the minimum residence time of suspended
233 particles in the estuary.

234
235 The concentration and Sr content of the suspended particulate load are summarized in Table 1.
236 The suspended load concentration is relatively constant and ranges from 492-650 mg/L in the
237 estuary. The Sr concentrations of this suspended particulate load also remain close to constant in
238 the mixing zone and ranges from 146-228 mg/kg. The $^{87}\text{Sr}/^{86}\text{Sr}$ ratios of these suspended
239 particles are illustrated as a function of the Cl concentration of their adjacent fluid in Fig. 3. In
240 contrast with the total concentration of the particles and their total Sr concentration, the $^{87}\text{Sr}/^{86}\text{Sr}$
241 ratios of the suspended particles show a dramatic shift towards seawater values in the estuary.

242
243 The chemical composition of the bedload samples collected during 2008 are listed in Table 2.
244 The $^{87}\text{Sr}/^{86}\text{Sr}$ ratios of these bedload samples are illustrated as a function of the Cl concentration
245 of their adjacent fluid in Fig. 3. The bedload sample $^{87}\text{Sr}/^{86}\text{Sr}$ ratios follow a similar trend as the

246 suspended particles but exhibit less of a seawater Sr isotope signal than the corresponding
 247 suspended particulate material. The Sr concentrations in the bedload increase away from the
 248 river mouth due to the presence of carbonate minerals (Jones et al., 2012a). That study
 249 concluded from mass balance equations that up to 14.9 % of the original basaltic Sr has been
 250 removed from the non-carbonate bedload.

251

252 **4. Discussion**

253 4.1 Estimation of the Sr fraction inputted to the estuary waters from particulate material

254 The degree to which Sr originating from particulate phases influences the estuarine water

255 chemistry can be estimated from mass balance calculations. By substituting $\left(\frac{^{87}\text{Sr}}{^{86}\text{Sr}}\right)_{2\text{comp}}$ for

256 $\left(\frac{^{87}\text{Sr}}{^{86}\text{Sr}}\right)_{\text{sample}}$ into Eqn. (1) and rearranging, one obtains:

257

$$258 \left(\frac{^{87}\text{Sr}}{^{86}\text{Sr}}\right)_x = \frac{\left(\frac{^{87}\text{Sr}}{^{86}\text{Sr}}\right)_{\text{sample}} - \left(F_{\text{river}} \times \left(\frac{^{87}\text{Sr}}{^{86}\text{Sr}}\right)_{\text{river}}\right)}{1 - F_{\text{river}}} \quad (3)$$

259 The difference between $\left(\frac{^{87}\text{Sr}}{^{86}\text{Sr}}\right)_x$ and $\left(\frac{^{87}\text{Sr}}{^{86}\text{Sr}}\right)_{\text{sw}}$ originates from a Sr source other than the

260 conservative mixing of river and sea water. It is assumed in this study that this difference occurs

261 from the conservative transfer of Sr from particulates to the fluid phase, and from the fluid to the

262 particulates. Taking account of this assumption, the fraction of the Sr present in the estuarine

263 water samples originating from particulate weathering (f_{part}) can then be obtained from:

264

265
$$f_{part} = \frac{\left(\frac{^{87}\text{Sr}}{^{86}\text{Sr}}\right)_x - \left(\frac{^{87}\text{Sr}}{^{86}\text{Sr}}\right)_{sw}}{\left(\frac{^{87}\text{Sr}}{^{86}\text{Sr}}\right)_{part} - \left(\frac{^{87}\text{Sr}}{^{86}\text{Sr}}\right)_{sw}} \quad (4)$$

266 where the subscript *part* designates the value of the particulate material, where the measured
 267 $\left(\frac{^{87}\text{Sr}}{^{86}\text{Sr}}\right)_{part} \approx 0.703294$. The total amount of Sr released from the particles to the fluid is attained
 268 by multiplying the dissolved Sr in the water by f_{part} ; the results of this calculation are provided in
 269 Supplementary Table 1. Note that the quantification of the particulate material release is
 270 severely hampered by the difference in element concentrations between the fresh and saline
 271 water. Consequently, the calculations either induce high errors at very low salinity levels, or are
 272 swamped by the seawater signature in high salinity areas. As such, f_{part} values are only reported
 273 over the $100 < \text{Sr} < 1000 \mu\text{g/L}$ concentration range. In this mid-mixing zone, measured $^{87}\text{Sr}/^{86}\text{Sr}$
 274 compositions require that an average $3.98 (\pm 2.7) \mu\text{g/L}$ of Sr be transferred from the particulates
 275 into the water. As these samples were collected at high tide, this Sr must have been liberated
 276 from the particulates to the seawater in a matter of minutes to hours.

277
 278 Similarly, mass balance calculations can be used to validate if the compositions of the suspended
 279 particle samples collected in 2011 are consistent with these being the source of the unradiogenic
 280 Sr required to balance the Sr composition of the estuary water. Taking account of mass balance
 281 constraints, the fraction of Sr in the particles originating from seawater (f_{sw}) can be calculated
 282 from:

283
 284
$$f_{sw} = \frac{\left(\frac{^{87}\text{Sr}}{^{86}\text{Sr}}\right)_{sample} - \left(\frac{^{87}\text{Sr}}{^{86}\text{Sr}}\right)_{basalt}}{\left(\frac{^{87}\text{Sr}}{^{86}\text{Sr}}\right)_{sw} - \left(\frac{^{87}\text{Sr}}{^{86}\text{Sr}}\right)_{basalt}} \quad (5)$$

285 where the subscripts *sample*, *basalt*, and *sw* refer to values for suspended particles in the estuary,
286 the basaltic Hvítá river end member, and the isotopic composition of seawater, respectively. As
287 the Sr concentrations in the particles are close to constant, the total mass of Sr transferred to the
288 estuarine waters from the particles ($m_{\text{Sr released}}$) is approximately:

$$290 \quad m_{\text{Sr released}} = f_{\text{sw}} \times m_{\text{Sr particles}} \quad (6)$$

291 where $m_{\text{Sr particles}}$ refers to the mass of Sr present in the particles. This assumes that the
292 provenance of the suspended material in the mixing zone is dominantly of terrestrial origin.
293 Therefore, these calculations were only performed up to sample Bo12 (64°34' N, 021°50' W).
294 The depth at Bo12 is <2 m and well within the confines of the estuary, which supports the
295 assumption that the overwhelming majority of suspended particulates in this part of the estuary
296 originate from the Hvítá catchment. This is also the final sample site used for estimating f_{part}
297 above. The seawater component (f_{sw}) is expressed as a percentage in Supplementary Table 1 and
298 Fig. 6 to provide a comparison with the estimates generated from the estuarine water
299 compositions.

300
301 The $^{87}\text{Sr}/^{86}\text{Sr}$ composition of the suspended load samples from 2011 indicates that <0.1 % of the
302 Sr in the suspended particles originated from seawater in the Hvítá River, but 86 % of the Sr in
303 suspended particles has a seawater signature at the Borgarfjörður Bridge. This observation
304 indicates that the transformation of the Sr isotopic compositions of the particles begins at very
305 low salinity levels (Fig. 6). Note that part of the isotopic evolution could be an artefact due to
306 contamination from residual salts on the filter, even after rinsing with deionized water.
307 However, the dramatic Sr isotopic evolution observed in the particulate material collected from

308 [the low salinity mixing zone, confirms that this effect is not an artefact of contamination.](#)
309 [Logically, one would expect that if there was any deviation from the dissolved mechanical](#)
310 [mixing line in the fjord, the particles would be more unradiogenic than their host water due to](#)
311 [resuspension through tidal action.](#)

312
313 The change in $^{87}\text{Sr}/^{86}\text{Sr}$ in the suspended particles while maintaining a near constant total Sr
314 concentration indicates the two way transfer of material from and into the particles. In total, the
315 [calculations presented above, based on the composition of the suspended particles collected in](#)
316 [2011, indicate that 9-27 \$\mu\text{g}/\text{L}\$ of Sr is transferred from the particles to the estuarine waters in the](#)
317 [mixing zone. This mass is 2.5-7.5 times greater than the input to seawater by dissolved riverine](#)
318 [transport and approximately 10-30 % of the total particulate Sr concentrations. Nevertheless,](#)
319 [these values are substantially greater than the corresponding estimates based on the analysis of](#)
320 [the concentrations of the estuary waters. The most likely reasons for this are a longer residence](#)
321 [time of particulates in the mixing zone compared to river water, and the formation of, and](#)
322 [exchange with Sr-bearing phases within the estuary. Nevertheless, the dramatic compositional](#)
323 [change in the suspended material](#) demonstrates that the particulate fraction is the major
324 contributor of Sr to estuarine waters through dissolution and/or exchange of Sr. The larger
325 [estimated](#) Sr release [deduced from](#) the suspended material compositions compared to that
326 indicated by the estuarine water compositions (1.1 times greater than the dissolved flux) may
327 reflect the larger residence time of the particulates in the mixing zone.

328

329 The question remains as to whether the Sr released from particulates is sourced by the
330 dissolution of [or exchange from](#) primary igneous minerals, secondary weathering phases, or even

331 colloids. Data from Hvítárvellir suggests that the Sr concentration of riverine colloids is far too
332 low (0.06 ng/g) for their flocculation to impact seawater chemistry. However, the Sr
333 concentration in Fe-Mn oxyhydroxides (1.8-2.4 $\mu\text{g/g}$) suggests that these phases may be a
334 significant source, consistent with the observed effects on $^{234}\text{U}/^{238}\text{U}$ activity ratios (Pogge von
335 Strandmann et al., 2008). Therefore, at least part of the two-way transfer of Sr between the
336 particulate and fluid phases could stem from adsorption-desorption processes, as shown by Li
337 isotopes (Pogge von Strandmann et al., 2008). Further insight into the mechanism responsible
338 for the reincorporation into the solid phase can be gained from Fig. 7, which illustrates the Sr/Al
339 ratio against the Ca/Al ratio for the bedload particulate material. These concentration ratios plot
340 as a near linear function of one another with a slope of 0.028. This dependence suggests that the
341 re-incorporation of Sr into the solids is due to its co-precipitation with Ca as the particulate
342 material interacted with seawater in the estuary. It seems likely that this precipitating phase is
343 calcite, given its high concentrations in these sediments (Pearce et al., 2013). The fact that this
344 linear correlation is offset from the origin by 0.6 Ca/Al implies that a substantial fraction of Sr in
345 the particulate material is hosted by non-carbonate phases (such as silicates).

347 4.2 Global Implications

348 These findings have far-reaching implications for the global element cycles. On a catchment
349 scale, the Hvítá River has a mean discharge of $89 \text{ m}^3 \text{ s}^{-1}$, with an annual particulate suspended
350 flux of 200,600 tons and a dissolved Sr flux of $9.54 \text{ tons yr}^{-1}$, based on monthly monitoring
351 (Eiriksdottir et al., 2011). The results described here indicate that a further $10.4\text{-}71.5 \text{ tons yr}^{-1}$ of
352 Sr will be transferred to the estuarine waters from particulates, assuming a linear covariance
353 between the dissolved and suspended flux throughout the year. In this case, the overall $^{87}\text{Sr}/^{86}\text{Sr}$

354 composition delivered to the ocean (both riverine dissolved and that from particulate dissolution)
355 is calculated to be between 0.70345 and 0.70391, rather than the value of 0.70459 of the riverine
356 dissolved signal alone. If this behaviour is typical for volcanic particulates worldwide, then
357 consideration of the geographic extent of volcanic islands and basaltic terrains (as defined by
358 Allègre et al., 2010 and Dessert et al., 2003) suggests from 42 and 291×10^9 g yr⁻¹ of Sr could be
359 released in this way. This release could account for between 6 and 45% of the current perceived
360 imbalance in the marine Sr budget, which is of comparable magnitude to the contribution from
361 hydrothermal exchange (Davis et al., 2003). [Estimations of annual fluxes based on summer spot
362 sampling from this catchment gave the dissolved Sr flux from Hvítá as 37 tons yr⁻¹ \(Pogge von
363 Strandmann et al., 2008\), underlining the sensitivity of these calculations to the conditions at the
364 time of sampling.](#) Crucially, these calculations only take into account the initial release of Sr in
365 the estuary; whereas reworking of the sediments is likely to continue to react over much longer
366 periods (e.g. Aller 1998), as exhibited by the experimental evidence (Jones et al., 2012a; 2012b;
367 Pearce et al., 2013).

368

369 While these results are conclusive field evidence of ‘proof of process’, there is some degree of
370 uncertainty associated with the magnitude of this flux, especially when scaled up to a global
371 process. Therefore, these may not necessarily be a fair reflection on the annual fluxes. There are
372 considerable climatic differences between Iceland and other basaltic provinces and outcrops
373 worldwide, which would result in varying degrees of weathering, soil formation, and denudation.
374 [Moreover, Iceland hosts several sub-glacial volcanoes that lead to the formation of significant
375 amounts of easily-weathered hyaloclastite \(hydrated tuff-like breccia that is rich in volcanic
376 glass, formed through water-lava interaction\).](#) Each of these variables would affect the partition

377 of Sr between the solid and fluid phases. Moreover, the relative contributions of mineral and
378 oxyhydroxide dissolution need to be more accurately quantified before firm flux estimates can be
379 made. Despite these uncertainties, the magnitude of these deviations in $^{87}\text{Sr}/^{86}\text{Sr}$ from a two
380 component mixing curve is clear evidence that the reactions of particulate material upon arrival
381 in coastal waters are a major contributor to the global cycle of Sr.

382

383 **5. Conclusions**

384 These results represent the first direct evidence that the weathering of riverine particulate
385 material upon arrival in coastal [areas](#) makes a significant contribution to the overall Sr chemistry
386 of seawater [over geological timescales](#). This is significant as marine $^{87}\text{Sr}/^{86}\text{Sr}$ values are a
387 default tool for estimating weathering rates over geological time. Moreover, this evidence
388 demonstrates that we may have underestimated the elemental mass of material being transferred
389 from the continents to the oceans. The feedback between climate and weathering is commonly
390 quantified based upon the mass of the alkali earth metals Ca and Mg transferred from the
391 continents to the oceans during weathering, which consume atmospheric CO_2 both during
392 chemical weathering and the precipitation of carbonates (e.g. Walker, et al., 1981; Berner et al.,
393 1983; Berner, 2004; Berner and Kothavala, 2001; Wallmann, 2001). If Ca and Mg behave in a
394 similar fashion to Sr, then the feedback between climate and weathering is stronger than
395 previously presumed ([Eiriksdottir et al., 2013](#)).

396

397 As the overwhelming mass of sparingly soluble bio-limiting nutrients such as Fe and P are
398 brought to the oceans in particulate form, the dissolution of these particulates in seawater could
399 provide a new stronger link between continental weathering and marine primary productivity.

400 Experimental [and field](#) studies demonstrate that elements such as Nd are similarly released from
401 particulate material into seawater, despite its preference for the solid phase ([e.g.](#) Pearce et al.,
402 2013; [Singh et al., 2012](#)). Such observations suggest that particulate weathering in estuaries is a
403 major contributor of these and other elements to seawater, lending weight to the “Boundary
404 Exchange” hypothesis where sediment-seawater reactions in shelf environments are a significant
405 source of the dissolved constituents in seawater (Jeandel, 1993; Lacan and Jeandel, 2005;
406 Jeandel et al., 2007; 2011; Siddall et al., 2008; Arsouze et al., 2009; Horikawa et al., 2011; Cater
407 et al., 2012; Wilson et al., 2012). These findings also add weight to previous studies, where
408 current land-to-ocean fluxes are proposed to be out of equilibrium following a recent
409 deglaciation (Vance et al., 2009). As glacial retreats expose substantial quantities of finely
410 ground material, the reactions of the particles in seawater provide an efficient mechanism for the
411 enhanced global weathering rates in addition to changes in the dissolved transport.
412 Anthropogenic changes to sediment fluxes through soil erosion and the damming of rivers are
413 likely to affect elemental and nutrient fluxes to coastal waters to a much greater extent than has
414 been previously considered, which may have deleterious consequences for coastal ecosystems.

415

416 **Acknowledgments**

417 [We are indebted to Jérôme Gaillardet and another anonymous reviewer for thorough and](#)
418 [constructive reviews.](#) We extend our thanks to Björgunarsveitin Brá, Emily Jones, Eydis
419 Eiríksdóttir, Haraldur Rafn Ingvason, Olivia Jones, Pierre Brunet, Rósa Ólafsdóttir, and Snorri
420 Guðbrandsson and for sampling and technical assistance. M.T.J. was supported by a Marie Curie
421 Intra-European Fellowship (PIEF-GA-2009-254495).

422

423 **References**

424 Albarède, F., Michard, A., Minster, J., Michard, G., 1981. $^{87}\text{Sr}/^{86}\text{Sr}$ ratios in hydrothermal
425 waters and deposits from the East Pacific Rise at 21°N. *Earth Planet. Sci. Lett.* 55, 229-
426 236.

427 Allègre, C., Louvat, P., Gaillardet, J., Meynadier, L., Rad, S., Capmas, F., 2010. The
428 fundamental role of island arc weathering in the oceanic Sr isotope budget. *Earth Planet.*
429 *Sci. Lett.* 292, 51–56.

430 Aller, R. 1998. Mobile deltaic and continental shelf muds as suboxic, fluidized bed reactors.
431 *Mar. Chem.* 61, 143-155.

432 Andersson, P.S., Wasserburg, G.J., Ingri, J., 1992. The sources and transport of Sr and Nd
433 isotopes in the Baltic Sea. *Earth Planet. Sci. Lett.* 113, 459-472.

434 Arsouze, T., Dutay, J.-C., Lacan, F., Jeandel, C., 2009. Reconstructing the Nd oceanic cycle
435 using a coupled dynamical-biogeochemical model. *Biogeosciences* 6, 1–18.

436 Bernat, M., Church, T., Allègre, C.J., 1972. Barium and strontium concentrations in Pacific and
437 Mediterranean seawater profiles by direct isotope dilution spectrometry. *Earth Planet.*
438 *Sci. Lett.* 16, 75-80.

439 Berner, R.A., 2004. *The Phanerozoic Carbon Cycle*. Oxford University Press, Oxford.

440 Berner, R.A., Kothavala, Z., 2001. GEOCARB III. A revised model of atmospheric CO₂ over
441 Phanerozoic time. *Am. J. Sci.* 301, 182-204.

442 Berner, R.A., Lasaga, A.C., Garrels, R.M., 1983. The carbonate-silicate geochemical cycle and
443 its effect on atmospheric carbon dioxide over the past 100 million years. *Am. J. Sci.* 283,
444 641-683.

445 Broecker, W.S., Peng, T.H., 1982. *Tracers in the Sea* (Eldigio Press, Lamont Doherty Geological
446 Observatory).

447 Cater, P., Vance, D., Hillenbrand, C.D., Smith, J.A., Shoosmith, D.R., 2012. The neodymium
448 isotopic composition of water masses in the eastern Pacific sector of the Southern Ocean.
449 *Geochim. Cosmochim. Acta*, 79, 41-59.

450 Davis, A., Bickle, M., Teagle, D., 2003. Imbalance in the oceanic strontium budget, *Earth*
451 *Planet. Sci. Lett.* 112, 173-187.

452 Dessert, C., Dupré, B., Gaillardet, J., François, L.M., Allègre, C.J., 2003. Basalt weathering laws
453 and the impact of basalt weathering on the global carbon cycle, *Chem. Geol.* 202, 257-
454 273.

455 Dupré, B., Dessert, C., Oliva, P., Goddérís, Y., Viers, J., François, L., Millot, R., Gaillardet, J.,
456 2003. Rivers, chemical weathering and Earth's climate. *C.R. Geosci.* 335, 1141-1160.

457 Eiriksdóttir, E.S., Gislason, S.R., Snorrason, Á., Harðardóttir, J., Þorlákssdóttir, S.B.,
458 Eyþórsdóttir, K.G., 2011. Efnasamsetning, Rennsli og Aurburður Straumvatna á
459 Vesturlandi V. Gagnagrunnur Jarðvísindastofnunar og Veðurstofunnar (Science Institute
460 Report 04, Háskóli Íslands).

461 Eiriksdóttir, E.S., Gislason, S.R., Oelkers, E.H., 2013. Does temperature or runoff control the
462 feedback between chemical denudation and climate? Insights from NE Iceland.
463 *Geochim. Cosmochim. Acta* 107, 65-81.

464 Elderfield, H. & Gieskes, J.M., 1982. Sr isotopes in interstitial waters of marine sediments from
465 Deep Sea Drilling Project cores, *Nature* 300, 493-497.

466 Elderfield, H., 1986. Strontium isotope stratigraphy. *Palaeogeogr. Palaeoclimatol. Palaeoecol.*
467 57, 71-90

468 Gislason, S.R., Arnórsson, S., Ármannsson, H., 1996. Chemical weathering of basalt in SW
469 Iceland: Effects of runoff, age of rocks and vegetative/glacial cover. *Am. J. Sci.* 296, 837-
470 907.

471 Gislason, S.R., Oelkers, E.H., 2003. The mechanism, rates and consequences of basaltic glass
472 dissolution: II. An experimental study of the dissolution rates of basaltic glass as a
473 function of pH and temperature. *Geochim. Cosmochim. Acta* 67, 3817-3832.

474 Gislason, S.R., Oelkers, E.H., Snorrason, A., 2006. Role of river-suspended material in the
475 global carbon cycle. *Geology* 34, 49-52.

476 Gudbrandsson, S., Wolff-Boenisch, D., Gislason, S.R., Oelkers, E.H., 2011. An experimental
477 study of crystalline basalt dissolution from $2 \leq \text{pH} \leq 11$ and temperatures from 5 to 75
478 °C. *Geochim. Cosmochim. Acta*, 75, 5496-5509.

479 Henderson, G.M., Martel, D.J., O’Nions, R.K., Shackleton, N.J., 1994. Evolution of seawater
480 $^{87}\text{Sr}/^{86}\text{Sr}$ over the last 400 ka: the absence of glacial/interglacial cycles, *Earth Planet. Sci.*
481 *Lett.* 128, 643–651.

482 Hodell, D., Mueller, P., McKenzie, J., Mead, G., 1989. Strontium isotope stratigraphy and
483 geochemistry of the late Neogene ocean, *Earth Planet. Sci. Lett.* 92, 165-178.

484 Horikawa, K., Martin, E.E., Asahara, Y., Sagawa, T., 2011. Limits on conservative behaviour of
485 Nd isotopes in seawater assessed from analysis of fish teeth from Pacific cores. *Earth*

486 Planet. Sci. Lett., 310, 119-130.

487 Jeandel, C. 1993. Concentration and isotopic composition of Nd in the South Atlantic Ocean.
488 Earth Planet. Sci. Lett. 117, 581-591.

489 Jeandel, C., Arsouze, T., F., Techine, P. and Dutay, J.C. 2007. Isotopic Nd compositions and
490 concentrations of the lithogenic inputs into the ocean: A compilation, with an emphasis on
491 the margins. Chem. Geol. 239, 156-164.

492 Jeandel, C., Peucker-Ehrenbrink, B., Jones, M.T., Pearce, C.R., Oelkers, E.H., Godderis, Y.,
493 Lacan, F., Aumont, O. and Arsouze, T. 2011. Ocean Margins: The missing term for
494 oceanic element budgets? EOS 92, 217-219.

495 Jones, M.T., Pearce, C.R., Oelkers, E.H., 2012a. An experimental study of the interaction of
496 basaltic riverine particulate material and seawater. Geochim. Cosmochim. Acta 77, 108-
497 120.

498 Jones, M.T., Pearce, C.R., Jeandel, C., Gislason, S.R., Eiriksdottir, E.S., Mavromatis, V., Oelkers,
499 E.H., 2012b. Riverine particulate material dissolution as a significant flux of strontium to
500 the oceans. Earth Planet. Sci. Lett. 355–356, 51–59.

501 Lacan, F., Jeandel, C., 2005. Neodymium isotopes as a new tool for quantifying exchange fluxes
502 at the continent-ocean interface. Earth Planet. Sci. Lett. 232, 245–257.

503 McArthur, J.M., Howarth, R.J., Bailey, T.R., 2001. Strontium Isotope Stratigraphy: LOWESS
504 Version 3: Best Fit to the Marine Sr-Isotope Curve for 0–509 Ma and Accompanying
505 Look-up Table for Deriving Numerical Age, *J. Geol.* **109**, 155-170.

506 Milliman, J.D., Farnsworth, K.L., 2011. River Discharge to the Coastal Ocean: A Global
507 Synthesis. Cambridge University Press.

508 Milliman, J.D., Syvitski, J., 1992. Geomorphic/tectonic control of sediment discharge to the
509 ocean: the importance of small mountainous rivers. *J. Geol.* 100, 525-544.

510 Oelkers, E.H., Gislason, S.R., Eiriksdottir, E.S., Jones, M.T., Pearce, C.R. and Jeandel, C. 2011.
511 The role of riverine particulate material on the global cycles of the elements. *Appl.*
512 *Geochem.* 26, S365-S369.

513 Oelkers, E.H., Gislason, S.R., Eiriksdottir, E.S., Jones, M.T., Pearce, C.R., Jeandel, C.,
514 2012. Riverine particulate material dissolution in seawater and its implications for the global
515 cycles of the elements. *C.R. Geosci.* 344, 646-651.

516 Oliver, L., Harris, N., Bickle, M., Chapman, H., Dise, N., Horstwood, M., 2003. Silicate
517 weathering rates decoupled from the $^{87}\text{Sr}/^{86}\text{Sr}$ ratio of the dissolved load during
518 Himalayan erosion. *Chem. Geol.*, 201 (1-2), 119-139.

519 Palmer, M., Edmond, J., 1989. The strontium isotope budget of the modern ocean, *Earth Planet.*
520 *Sci. Lett.* 92, 11-26.

521 Palmer, M. R., Edmond, J. M., 1992, Controls over the strontium isotope composition of river
522 water: *Geochim. Cosmochim. Acta*, 56, 2099–2111.

523 Pearce, C.R., Burton, K.W., Pogge von Strandmann, P.A.E., James, R.H., Gislason, S.R., 2010.
524 Molybdenum isotope behaviour accompanying weathering and riverine transport in a
525 basaltic terrain. *Earth Planet. Sci. Lett.* 295, 104-114.

526 Pearce, C.R., Jones, M.T., Oelkers, E.H., Pradoux, C., Jeandel, C., 2013. The effect of
527 particulate dissolution on the neodymium (Nd) isotope and Rare Earth Element (REE)
528 composition of seawater. *Earth Planet. Sci. Lett.* 369, 138-147

529 Peucker-Ehrenbrink, B., Miller, M.W., Arsouze, T., Jeandel, C., 2010. Continental bedrock and
530 riverine fluxes of strontium and riverine particulate material dissolution in seawater
531 neodymium isotopes to the oceans. *Geochem. Geophys. Geosy.* 11, Q03016.

532 Pogge von Strandmann, P.A.E., James, R.H., van Calsteren, P., Gislason, S.R., Burton, K.W.,
533 2008. Lithium, magnesium and uranium isotope behaviour in the estuarine environment
534 of basaltic islands. *Earth Planet. Sci. Lett.* 274, 462-471.

535 Riley, J.P., Chester, R., 1971. *Introduction to Marine Chemistry*. Academic Press, London.

536 Siddall, M., Khatiwala, S., van der Fliedert, T., Jones, K., Goldstein, S.L., Hemming, S.,
537 Anderson, R.F., 2008. Towards explaining the Nd paradox using reversible scavenging in
538 an ocean general circulation model. *Earth Planet. Sci. Lett.* 274, 448-461.

539 Singh, S.P., Singh, S.K., Goswami, V., Bhushan, R., Rai, V.K., 2012. Spatial distribution of
540 dissolved neodymium and ϵ_{Nd} in the Bay of Bengal: Role of particulate matter and
541 mixing of water masses. *Geochim. Cosmochim. Acta*, 94, 38-56.

542 Vance, D., Teagle, D., Foster, G., 2009. Variable Quaternary chemical weathering fluxes and
543 imbalances in marine geochemical budgets, *Nature* 458, 493-496.

544 Veizer, J., Alab, D., Azmy, K., Bruckschen, P., Buhl, D., Bruhn, F., Cardena, G.A.F., Diener, A.,
545 Ebner, S., Godderis, Y., Jasper, T., Korte, C., Pawellek, F., Podlaha, O.G., Strauss, H.,
546 1999. $^{87}Sr/^{86}Sr$, ^{13}C and ^{18}O evolution of Phanerozoic seawater. *Chem. Geol.* 161, 59-88.

547 Walker, J.C.G., Hays, P.B., Kasting, J.F., 1981. A negative feedback mechanism for the long-
548 term stabilization of Earth's surface temperature. *J. Geophys. Res.* 86, 9776-9782.

549 Walling, D.E., 2006. Human impact on land-ocean sediment transfer by the world's rivers.
550 *Geomorphology* 79, 192-216.

551 Wallmann, K., 2001. Controls on the Cretaceous and Cenozoic evolution of seawater
552 composition, atmospheric CO₂ and climate. *Geochim. Cosmochim. Acta* 65, 3005-3025.

553 Wilson D.J., Piotrowski, A.M., Galy. A., McCave N., 2012. A boundary exchange influence on
554 deglacial neodymium isotope records from the deep western Indian Ocean. *Earth. Planet.*
555 *Sci. Let.*, 341-344, 36-47.

556 Wolf-Boenisch, D., Gislason, S.R., Oelkers, E.H., Putnis, C.V., 2004. The dissolution rates of
557 natural glasses as a function of their composition at pH 4 and 10.6, and temperatures from
558 25 to 74 °C. *Geochim. Cosmochim. Acta* 68, 4843-4858.

559

560 **Legends**

561 **Fig. 1.** A map of western Iceland, showing the sample locations in the Hvítá River and the
562 Borgarfjörður Estuary. The 2003 ([black circles](#)) and 2011 ([grey circles](#)) transects collected
563 dissolved and suspended samples. The 2003 samples correspond to A4 and C1-11 from previous
564 studies (Pogge von Strandmann et al., 2008). The 2008 transect (black triangles) collected
565 bedload samples.

566

567 [Fig. 2.](#) A log-log comparison of dissolved [Sr] and [Cl] concentrations measured in the 2011
568 samples ([grey circles](#)) and 2003 samples ([black circles](#)). The black line represents the pure
569 [mechanical mixing line between the seawater and river water end-members, with the grey shaded](#)
570 [area representing the error on this line due to uncertainties associated with the true riverine end-](#)
571 [member.](#)

572

573 | **Fig. 3.** The measured $^{87}\text{Sr}/^{86}\text{Sr}$ from the dissolved (grey circles) and suspended (grey squares)
574 | samples from 2011, and bedload (black triangles) fractions from 2008 against estuarine water
575 | dissolved chloride concentrations. The solid curves represent the predicted $^{87}\text{Sr}/^{86}\text{Sr}$ from
576 | mechanical two-component mixing of the riverine and seawater end-members, with associated
577 | measurement and analytical errors of this line represented by the grey area within the dashed
578 | lines. Errors for individual points are well within the size of the symbols.

579 |
580 | **Fig. 4.** The measured $^{87}\text{Sr}/^{86}\text{Sr}$ compared with the fraction of river-derived [Sr] concentrations.
581 | As with Fig. 2, the black line represents the seawater – river water mechanical mixing line, with
582 | the grey shaded area representing the error on this line due to analytical uncertainties.

583 |

584 | **Fig. 5.** The difference between the observed $^{87}\text{Sr}/^{86}\text{Sr}$ in dissolved field estuarine water samples
585 | and the calculated $^{87}\text{Sr}/^{86}\text{Sr}$ ratios at a given Cl concentration, based on mechanical two-
586 | component mixing (corresponding to the curve in Fig. 2). The model curves represent the
587 | calculated deviations from this mechanical mixing, based on experimental release rates from
588 | Hvítá bedload (Jones et al., 2012a) and suspended particulates from northeast Iceland (Jones et
589 | al., 2012b) in seawater after 1-4 days.

590 |

591 | **Fig. 6.** The estimated % seawater signal between the suspended particles (based on $^{87}\text{Sr}/^{86}\text{Sr}$) and
592 | dissolved [Cl] concentrations from the same sample. [Sr] vs [Cl] concentrations are shown for
593 | comparison.

594 |

595 | [Fig. 7. The Sr/Al concentration ratios plotted against the corresponding Ca/Al concentration](#)
596 | [ratios of the bedload particulate material. The symbols correspond to measured concentrations](#)
597 | [while the line represents the least squares fit of the data.](#)
598 |

599 | **Table 1.** Location and chemical data of the water and suspended samples collected in 2011 and
600 | 2003. n.a. denotes “not analysed” and b.d.l. denotes “below detection limit”.

601 |

602 | **Table 2.** The chemical data of the bedload samples collected in 2008. The “corresponding site”
603 | labels match those used in Pogge von Strandmann et al. (2008). * denotes that all Fe is assumed
604 | to be as Fe³⁺.

605 |

606 | **Supplementary Information**

607 | Supplementary Table 1 is a summary of the analyses that calculated the relative release of Sr,
608 | based on equations 1-6.

Highlights (for review)

- We conducted a suite of field investigations in Borgarfjörður estuary in west Iceland.
- Dissolved, suspended and bedload $^{87}\text{Sr}/^{86}\text{Sr}$ values show clear Sr release from particulates.
- Magnitudes of Sr dissolution agree with experimentally derived values.
- Sr release from sediments must occur within hours of first contact with saline water.
- Global Sr flux estimates of comparable magnitude to mid-ocean ridge Sr exchange.

Figure
[Click here to download high resolution image](#)

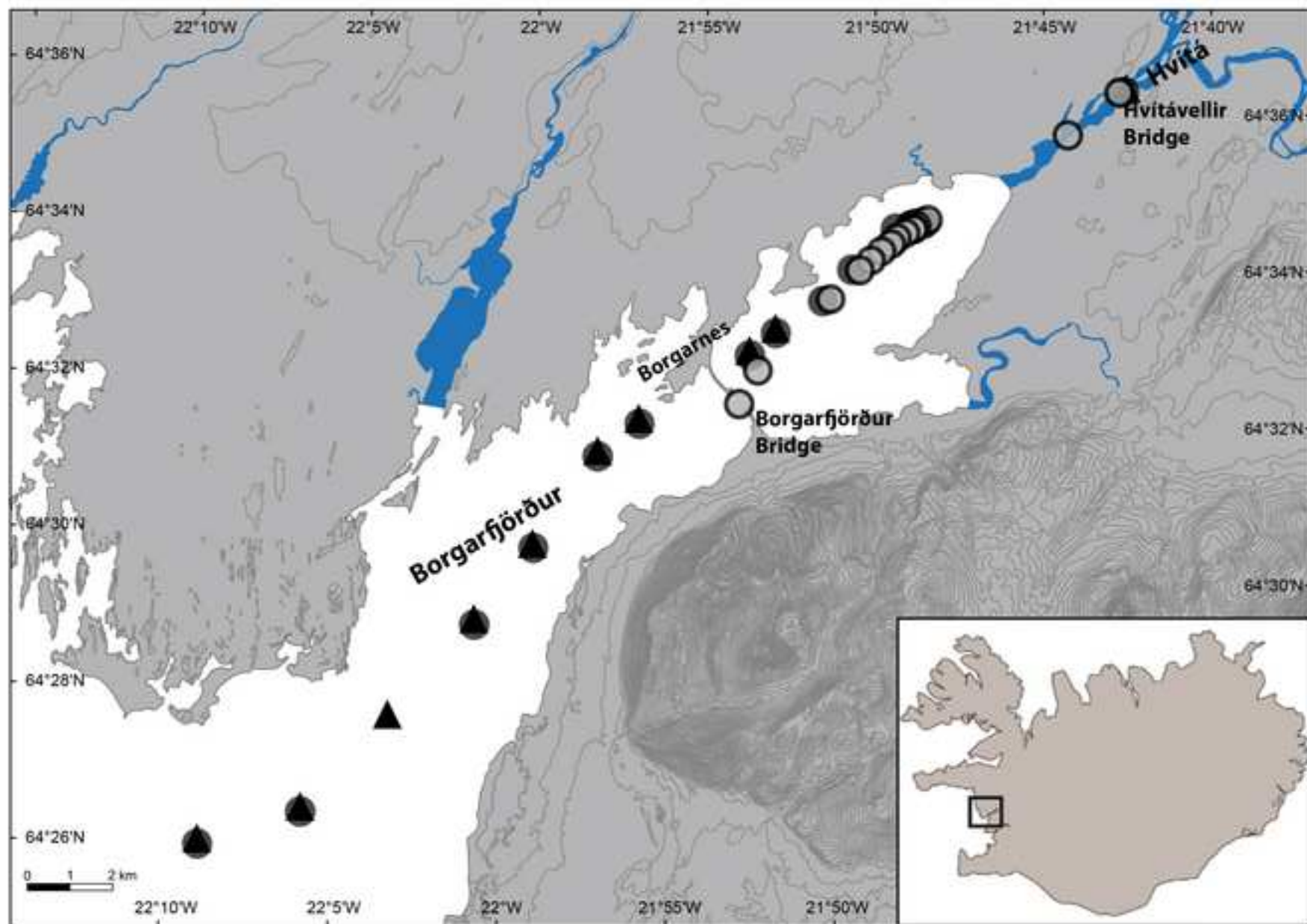


Figure
[Click here to download high resolution image](#)

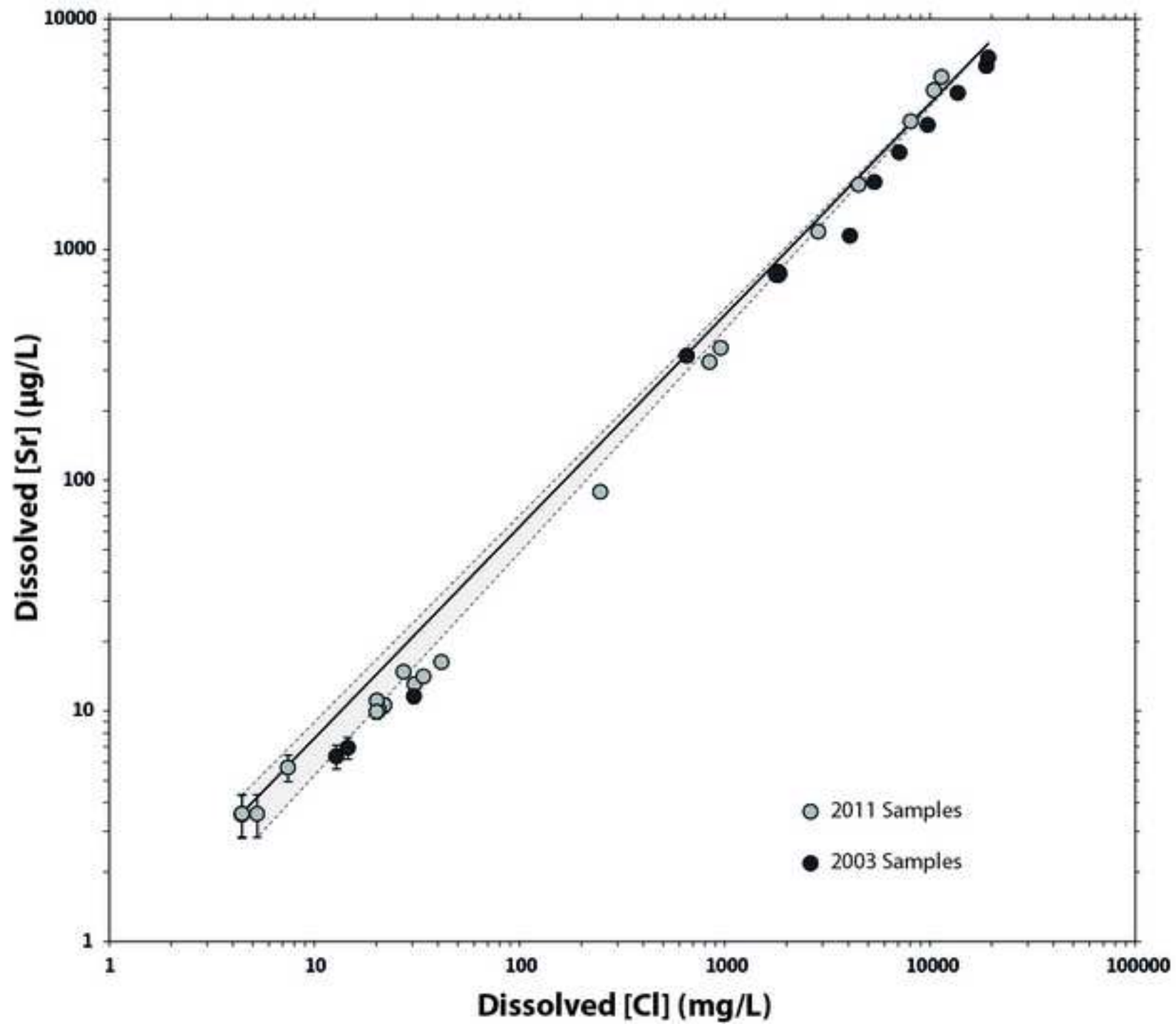


Figure
[Click here to download high resolution image](#)

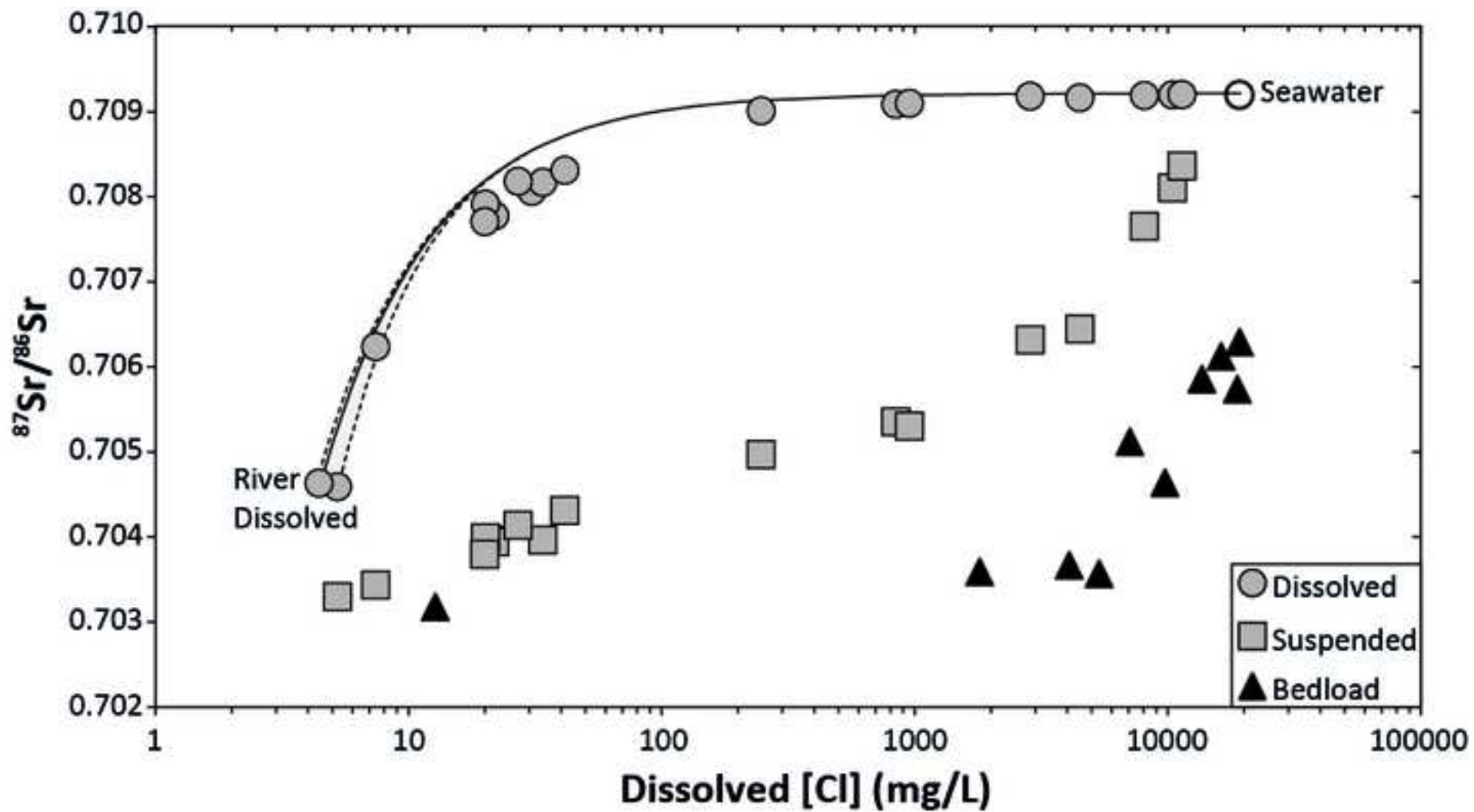


Figure
[Click here to download high resolution image](#)

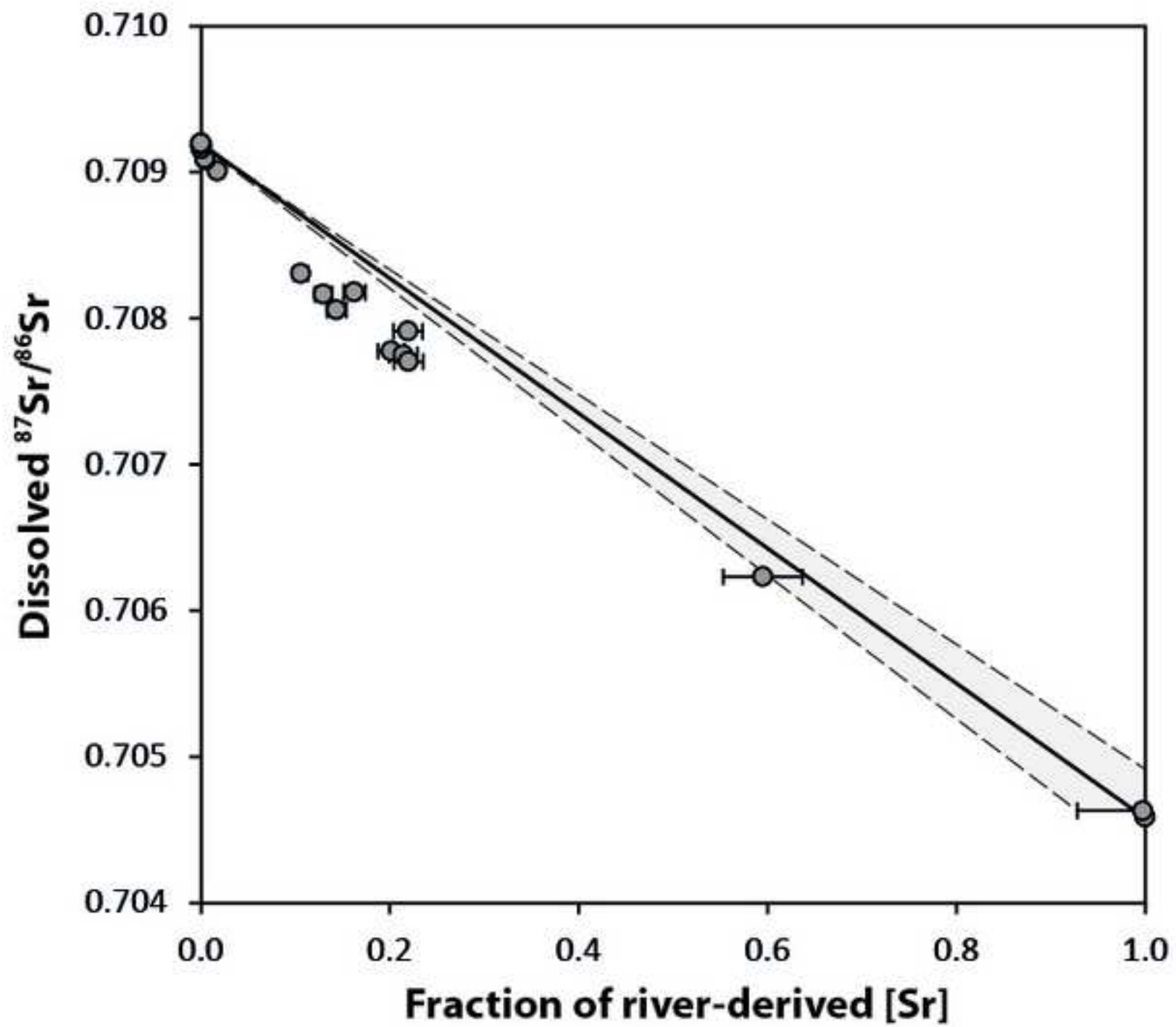


Figure
[Click here to download high resolution image](#)

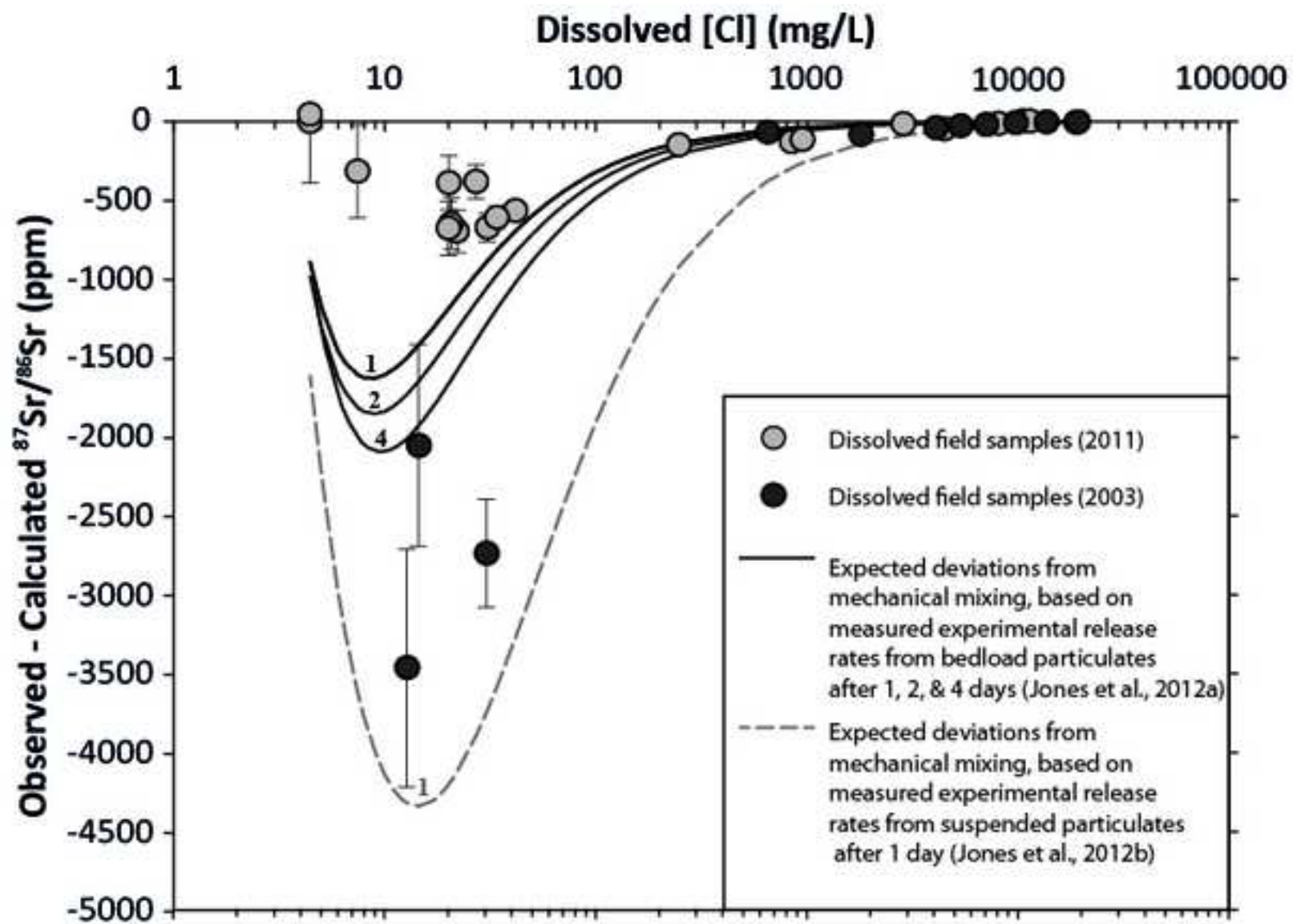


Figure
[Click here to download high resolution image](#)

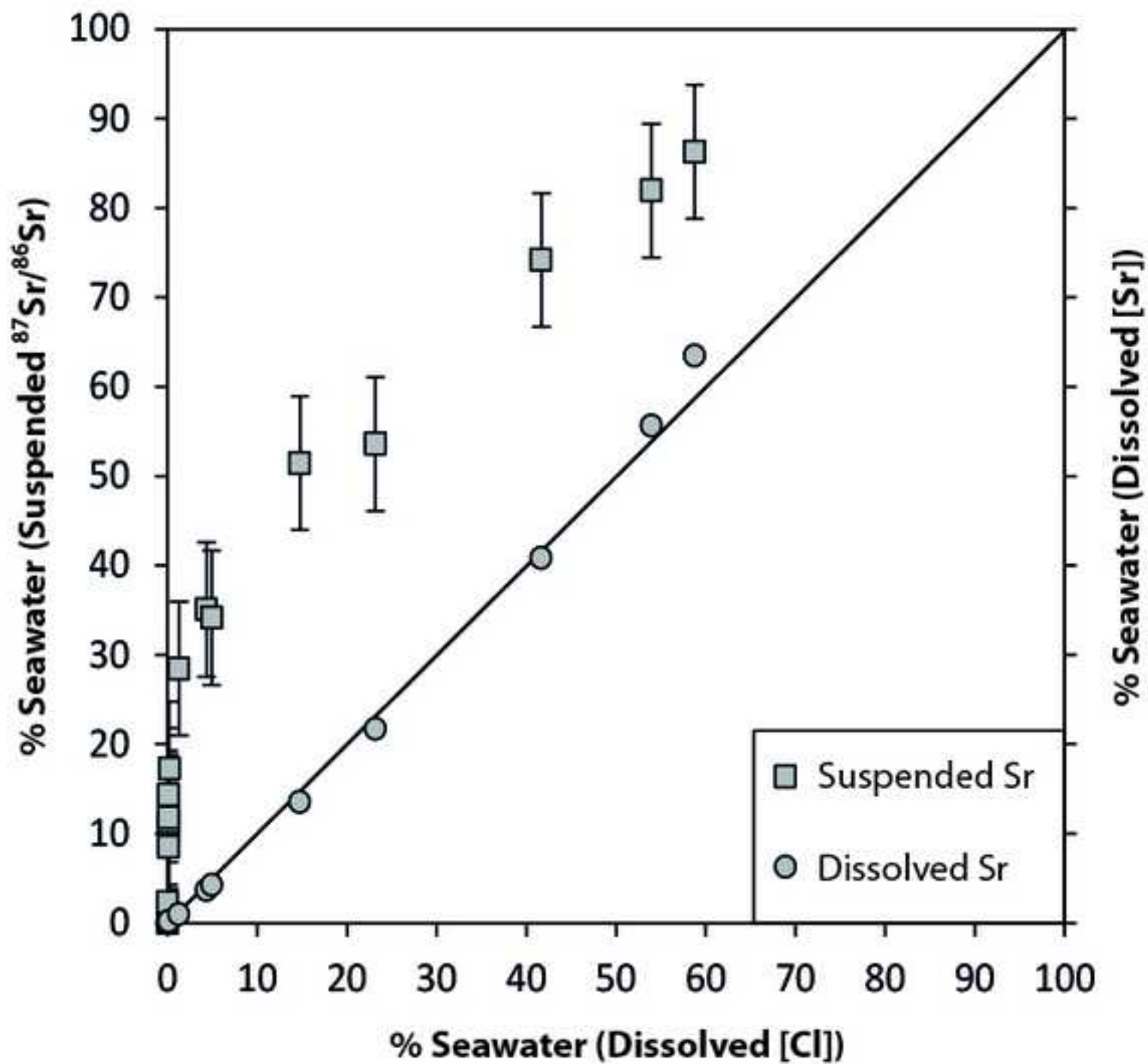


Figure
[Click here to download high resolution image](#)

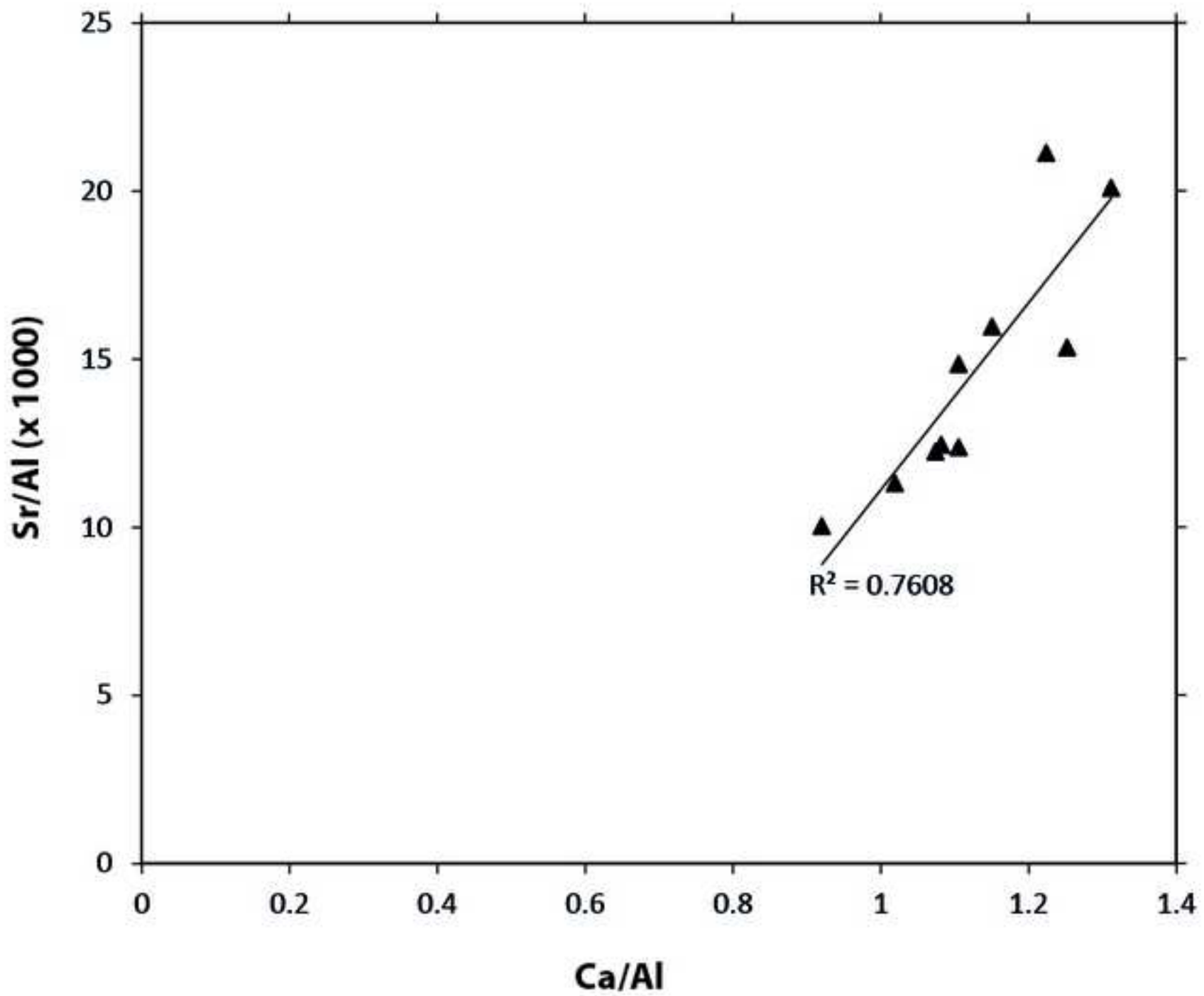


Table
[Click here to download Table: Table 1.xlsx](#)

Site	Latitude	Longitude	Date	Time	Distance from Hvitávellir	Water Temp.	pH	Conductivity	Salinity	Suspended Fraction	Alkalinity	Cl	SO ₄	Si	Na	K	Ca	Mg	Fe	Al	Mn	Li	Br	B	Sr	Dissolved ⁸⁷ Sr/ ⁸⁶ Sr	Suspended Sr	Suspended ⁸⁷ Sr/ ⁸⁶ Sr
					km	°C	mS	% of S.W.		mg/L	meq/L	mg/L	mg/L	mg/L	mg/L	mg/L	mg/L	mg/L	mg/L	µg/L	µg/L	µg/L	mg/L	mg/L	µg/L		mg/kg	
HvA	64°36'11.0"	021°42'37.5"	25/08/2011	14:55	0.00	7.7	8.08	0.06	0.03	562	0.390	5.3	0.4	6.51	6.7	0.5	3.1	1.1	0.022	71.5	1.67	0.18	0.014	0.005	3.6	0.704589	228.3	0.703294
HvB	64°36'11.0"	021°42'37.5"	25/08/2011	15:25	0.00	7.6	8.08	0.07	0.02	560	0.385	4.4	0.2	6.43	6.6	0.4	3.0	1.1	0.008	61.3	1.16	0.14	0.013	0.004	3.6	n.a	n.a	n.a
Bo1	64°35'36.8"	021°44'06.5"	25/08/2011	16:10	1.57	7.5	8.08	0.06	0.02	507	0.393	4.4	0.2	6.29	6.9	0.4	3.0	1.1	0.009	59.9	0.57	0.17	0.003	0.003	3.6	0.704631	177.9	n.a
Bo6	64°34'27.1"	021°48'09.7"	25/08/2011	17:00	5.43	8.6	7.81	0.08	0.04	505	0.450	7.4	0.8	6.38	8.7	0.5	3.1	1.4	0.013	61.0	1.95	0.23	0.014	0.005	5.7	0.706233	159.2	0.703430
Bo2	64°34'24.1"	021°48'16.7"	25/08/2011	16:40	5.54	9.5	7.80	0.07	0.16	506	0.402	30.7	5.5	6.50	21.3	1.0	3.1	2.6	0.009	51.0	4.97	0.56	0.074	0.015	13.1	0.708060	180.3	n.a
Bo5	64°34'25.0"	021°48'21.2"	25/08/2011	16:55	5.60	9.8	7.81	0.14	0.11	499	0.406	21.9	3.9	6.46	16.9	0.9	3.1	2.2	0.013	52.0	4.46	0.45	0.072	0.009	10.6	0.707776	174.9	0.703940
Bo7	64°34'22.4"	021°48'29.4"	25/08/2011	17:05	5.72	9.5	7.78	0.24	0.21	486	0.407	41.6	7.8	6.51	27.6	1.3	3.3	3.2	0.010	52.1	4.29	0.74	0.123	0.018	16.3	0.708309	163.5	0.704309
Bo4	64°34'23.7"	021°48'32.2"	25/08/2011	16:52	5.73	9.5	7.81	0.13	0.11	501	0.396	20.6	3.5	6.49	16.0	0.8	3.0	2.1	0.009	49.8	3.55	0.75	0.063	0.008	10.2	0.707751	175.2	n.a
Bo3	64°34'22.6"	021°48'39.3"	25/08/2011	16:50	5.82	9.9	7.82	0.27	0.18	505	0.460	34.0	6.1	6.41	23.9	1.1	3.1	2.8	0.011	50.5	4.41	0.62	0.112	0.014	14.2	0.708167	180.3	0.703960
Bo8	64°34'19.6"	021°48'34.9"	25/08/2011	17:10	5.83	9.8	7.78	0.14	0.10	489	0.401	20.1	4.3	6.56	18.0	1.1	3.1	2.4	0.020	62.4	4.51	0.84	0.077	0.010	11.1	0.707912	151.8	0.703987
Bo8-bottom	64°34'19.6"	021°48'34.9"	25/08/2011	17:12	5.83	9.6	7.77	0.13	0.10	747	0.400	20.1	3.4	6.54	15.6	0.8	3.0	2.1	0.011	52.1	2.84	0.17	0.072	0.009	10.0	0.707705	299.0	0.703795
Bo9	64°34'16.3"	021°48'48.7"	25/08/2011	17:15	6.04	9.6	7.78	0.18	0.14	493	0.453	27.2	6.1	6.74	22.6	1.1	3.3	3.1	0.019	61.0	3.26	0.82	0.104	0.012	14.8	0.708179	155.8	0.704135
Bo10	64°34'12.1"	021°49'03.2"	25/08/2011	17:20	6.26	9.6	7.77	0.93	1.28	492	0.431	247.6	24.7	6.45	131.0	5.4	7.4	16.1	0.014	55.8	3.93	8.17	0.739	0.061	89.2	0.709010	151.9	0.704966
Bo11	64°34'07.5"	021°49'13.6"	25/08/2011	17:25	6.45	9.3	7.81	3.62	4.35	494	0.492	843.5	174.6	6.18	471.0	18.0	21.0	57.4	0.010	48.5	4.14	8.39	2.622	0.213	326.0	0.709083	157.1	0.705353
Bo12	64°34'01.5"	021°49'29.4"	25/08/2011	17:29	6.74	9.5	7.84	4.14	4.92	496	0.502	954.8	183.7	6.12	578.0	20.6	23.9	66.5	0.009	49.4	5.02	9.88	3.314	0.238	376.0	0.709095	145.9	0.705300
Bo13	64°33'54.2"	021°49'47.6"	25/08/2011	17:32	7.05	9.5	7.98	n.a	14.75	499	0.770	2861.2	574.4	5.37	1700.0	65.1	70.4	213.0	0.005	41.8	7.86	21.10	10.427	0.715	1200.0	0.709180	202.3	0.706315
Bo14	64°33'46.4"	021°50'07.1"	25/08/2011	17:36	7.41	9.9	8.00	n.a	23.19	517	0.901	4498.2	980.1	4.62	2880.0	102.0	111.0	336.0	b.d.l	36.2	8.64	54.83	17.023	1.113	1920.0	0.709161	150.1	0.706441
Bo15	64°33'23.0"	021°50'56.7"	25/08/2011	17:40	8.36	10.1	8.11	n.a	41.67	651	1.389	8084.8	n.a	3.06	5550.0	199.0	205.0	642.0	0.005	18.1	8.00	85.64	31.602	2.179	3610.0	0.709186	146.5	0.707647
Bo16	64°32'26.0"	021°53'00.8"	25/08/2011	17:45	10.74	10.6	8.12	n.a	53.92	n.a	1.623	10460.9	n.a	2.08	7450.0	268.0	278.0	861.0	b.d.l	12.0	7.32	109.19	43.646	3.019	4920.0	0.709197	143.9	0.708104
Bo17	64°31'59.6"	021°53'31.2"	25/08/2011	17:52	11.57	10.5	8.08	n.a	58.78	n.a	1.836	11402.8	n.a	1.50	8460.0	306.0	315.0	977.0	b.d.l	10.6	6.95	111.30	48.553	3.620	5610.0	0.709198	139.1	0.708359

Site	Latitude	Longitude	Date	Time	Distance from Hvitávellir	Temp.	pH	Conductivity	Salinity	Suspended Fraction	Alkalinity	TDS	Cl	SO ₄	Na	K	Ca	Mg	Li	Sr	Dissolved ⁸⁷ Sr/ ⁸⁶ Sr	Suspended Sr	Suspended ⁸⁷ Sr/ ⁸⁶ Sr	Colloid Sr	Colloid ⁸⁷ Sr/ ⁸⁶ Sr	Suspended Fe-Mn Leachate Sr	Suspended Fe-Mn Leachate ⁸⁷ Sr/ ⁸⁶ Sr
					km	°C	mS	% of S.W.		mg/L	meq/L	mg/L	mg/L	mg/L	mg/L	mg/L	mg/L	mg/L	µg/L	mg/L		mg/kg		mg/kg			
A4	N 64°36.199'	W 21°42.481'	09/09/2003	09:30	0.00	9.0	7.93	0.07	0.1	610	0.473	34.7	12.8	0.5	7.1	0.5	3.9	1.9	0.3	6.4	0.705155	192	0.703344	0.00056	0.704567	1.78	0.704555
C1	N 64°34.290'	W 21°49.299'	09/09/2003	08:20	6.43	7.7	7.92	0.07	0.2	n.a	n.a	33.4	14.5	0.8	7.5	0.5	4.2	6.4	0.3	6.9	0.706343	n.a	0.703347	n.a	n.a	n.a	n.a
C2	N 64°33.584'	W 21°51.107'	09/09/2003	08:40	8.42	8.0	7.95	0.09	0.2	n.a	n.a	47.2	30.5	1.0	12.9	0.7	4.3	2.0	0.4	11.6	0.706593	n.a	0.703485	n.a	n.a	n.a	n.a
C3	N 64°33.207'	W 21°51.792'	09/09/2003	09:10	9.21	8.8	7.94	2.89	5.4	n.a	n.a	1419	652.3	218.1	547.2	25.0	26.8	2.7	9.4	346.6	0.709118	210	0.706838	n.a	n.a	n.a	n.a
C4	N 64°32.924'	W 21°52.529'	09/09/2003	09:45	10.00	9.4	8.08	7.15	13.3	n.a	n.a	3570	1808.1	309.3	1142.6	51.6	51.7	67.1	21.0	788.5	0.709127	201	0.707744	n.a	n.a	n.a	n.a
C5	N 64°32.623'	W 21°53.270'	09/09/2003	10:00	10.84	9.6	8.16	9.81	19.1	n.a	n.a	4900	4077.1	576.3	1676.0	75.9	72.5	139.0	30.3	1147.8	0.709166	195	0.708191	n.a	n.a	n.a	n.a
C6	N 64°31.686'	W 21°56.450'	09/09/2003	10:10	13.94	9.8	8.22	12.91	24.8	n.a	n.a	6460	5353.4	714.7	2666.8	118.5	113.8	325.7	48.0	1962.7	0.709176	199	0.708359	n.a	n.a	n.a	n.a
C7	N 64°31.240'	W 21°57.647'	09/09/2003	10:30	15.18	10.4	8.25	15.27	29.7	n.a	n.a	7660	7090.6	810.7	3747.3	162.3	156.7	454.5	71.5	2637.4	0.709182	212	0.708505	n.a	n.a	n.a	n.a
C8	N 64°30.035'	W 21°59.427'	09/09/2003	10:40	17.71	10.7	8.27	21.79	41.2	n.a	n.a	10930	9749.6	1075.8	4758.9	198.6	194.8	578.5	90.2	3469.8	0.709191	n.a	n.a	n.a	n.a	n.a	n.a
C9	N 64°29.019'	W 22°01.071'	09/09/2003	11:05	19.90	11.1	8.28	30.80	58.6	n.a	n.a	15400	13649.4	1488.9	6713.0	283.1	276.6	806.9	121.5	4775.3	0.709194	77.9	0.708576	n.a	n.a	n.a	n.a
C10	N 64°26.523'	W 22°05.955'	09/09/2003	11:20	25.94	11.8	8.26	44.20	87.2	n.a	n.a	21700	18825.5	2218.9	9149.9	406.6	381.2	1125.3	155.5	6247.3	0.709194	n.a	n.a	n.a	n.a	n.a	n.a
C11	N 64°26.050'	W 22°08.966'	09/09/2003	11:45	28.33	12.1	8.29	47.10	90.6	n.a	n.a	23500	19215.5	2286.2	9632.7	422.3	404.8	1183.7	163.1	6799.3	0.709194	14.2	0.708699	n.a	n.a	n.a	n.a

Table

[Click here to download Table: Table 2.xlsx](#)

2008 Bedload	Bed 1	Bed 2	Bed 3	Bed 4	Bed 5	Bed 6
Corresponding site	A4	C4	C5	C6	C7	C8
Lat.	N 64°36.199'	N 64°32.924'	N 64°32.623'	N 64°31.686'	N 64°31.240'	N 64°30.035'
Long.	W 21°42.481'	W 21°52.529'	W 21°53.270'	W 21°56.450'	W 21°57.647'	W 21°59.427'
BET (m ² g ⁻¹)	6.358	11.14	9.603	9.756	12.38	8.404
SiO ₂ (%)	46.74	46.29	45.81	46.82	44.94	45.30
Na ₂ O (%)	2.67	2.40	2.19	2.28	2.72	2.20
MgO (%)	8.17	9.00	9.00	8.51	7.20	9.75
Al ₂ O ₃ (%)	15.24	13.06	13.07	13.70	13.24	11.46
P ₂ O ₅ (%)	0.14	0.12	0.13	0.12	0.17	0.13
K ₂ O (%)	0.28	0.39	0.33	0.38	0.49	0.38
CaO (%)	14.02	14.02	14.14	13.96	14.63	14.35
TiO ₂ (%)	1.45	1.49	1.56	1.44	1.49	1.57
MnO (%)	0.24	0.20	0.20	0.19	0.16	0.18
Fe ₂ O ₃ * (%)	10.81	11.46	11.90	11.52	12.42	12.99
Sr (mg kg ⁻¹)	152.90	159.94	162.64	154.90	196.53	175.92
⁸⁷ Sr/ ⁸⁶ Sr	0.703180	0.703591	0.703668	0.703569	0.705118	0.704637

Supplementary material for on-line publication only

[Click here to download Supplementary material for on-line publication only: Supplementary Table 1.xlsx](#)